Solid-State Electronics 197 (2022) 108463

Contents lists available at ScienceDirect

Solid State Electronics

journal homepage: www.elsevier.com/locate/sse

Correlation of natural honey-based RRAM processing and switching properties by experimental study and machine learning

Brandon Sueoka, Abdi Yamil Vicenciodelmoral, Md Mehedi Hasan Tanim, Xinghui Zhao *, Feng Zhao *

School of Engineering and Computer Science, Washington State University, Vancouver, WA 98686, United States

ARTICLE INFO

The review of this paper was arranged by "ED-Kuniyuki Kakushima"

Keywords:
Honey
Nonvolatile memory
Artificial synaptic device
Neuromorphic systems
Resistive switching memory
Machine learning

ABSTRACT

Natural honey is a promising material for hardware components of nonvolatile memory and artificial synaptic devices in emerging renewable and biodegradable neuromorphic systems. The resistive switching properties of these devices are closely correlated with device process conditions. In this paper, honey based resistive random access memory (RRAM) devices were fabricated with different metal electrodes and drying temperature and duration. SET and RESET voltages were measured and used as dataset to train machine learning algorithms. Four machine learning models were applied to process data and demonstrated an average accuracy of 89.9 % to 91.6 % to predict the SET voltages in the range of [0 V, 6 V]. This study established a useful practice for fabrication of RRAM devices based on honey and can be extended to other natural organic materials.

1. Introduction

Nonvolatile memory device is an essential hardware unit for information processing and data storage in emerging neuromorphic systems. Nonvolatile memory devices based on phase change memory [1], resistive switching memory [2], electrochemical devices [3], 2D devices [4], etc. have been demonstrated. Among these device technologies, resistive random access memory (RRAM) has been identified as a promising technology. A variety of natural organic materials mainly from protein and polysaccharide such as silk [5], gelatRRAMin [6], albumen [7], chitosan [8], cellulose nanofiber [9], starch [10], Aloe vera [11], glucose [12], fructose [13], etc. have demonstrated resistive switching properties. However, one of the challenges in the development of RRAM based on natural organic materials is that the resistive switching property is a strong reliance on process conditions [11] of the resistive switching thin film and electrode materials.

In this paper, we report a new approach to efficiently correlate natural organic RRAM process conditions with resistive switching characteristics by both experimental study and machine learning. Specifically, the film process conditions, film properties and device characteristics collected by experimental study were used as dataset to train machine learning algorithms, which was then able to make predictions and optimization on process condition. The natural material used for this study was honey, a natural sweet product [14] represented mainly by sugar, i.e. monosaccharides and disaccharides. Recently we have developed RRAM devices based on honey with promising bipolar resistive switching characteristics [15–17]. In this study, honey thin films were fabricated by a solution process with different process conditions of drying temperature and duration, and different bottom electrodes for comparison. SET and RESET voltages of honey-based RRAMs were tested and their values were correlated with process conditions. These process parameters and test results were used as training data for machine learning algorithm. Instead of many "trial and error" fabrication and testing cycles, machine learning can be utilized to more accurately and efficiently optimize the fabrication process.

2. Experimental

Five glass slides were used as the substrates of honey-RRAMs and cleaned in acetone, isopropyl alcohol and deionized water (D.I. water), each for 10 mins in an ultrasonic bath. Cu film was deposited on 2 slides and ITO was deposited on 3 slides by sputtering (Kurt Lesker Nano36). Honey solution was prepared by mixing commercially purchased honey in D.I. water with a 30 % concentration by weight. The solution was kept in a vacuum desiccator for overnight to make sure honey is dissolved completely in water and no air bubbles exist in the solution. Spin coating

* Corresponding authors.
E-mail addresses: x.zhao@wsu.edu (X. Zhao), feng.zhao@wsu.edu (F. Zhao).

https://doi.org/10.1016/j.sse.2022.108463
Received 2 May 2022; Received in revised form 10 August 2022; Accepted 14 September 2022
Available online 20 September 2022

at 3000 rpm for 90 s was applied to coat the honey film on all 5 samples, followed by baking on a hotplate at different temperatures and durations. During baking, Cu film was oxidized to Cu_xO to form Cu_xO/Cu bottom electrode (BE) while ITO BE doesn't change since it is thermal stable. Final Al film was deposited by sputtering through a stencil mask with circular opening windows on the dried honey film to form top electrode (TE). Fig. 1 showed the process flow, photographs of two samples after fabrication, and sample numbers with process conditions.

Resistive switching characteristics were measured in air and at room temperature on a Signatone probe-station. A Keithley 4200 semiconductor characterization system was used to supply voltage sweeps and measure currents in the devices. The bias voltages were applied on the TE of the honey devices while the BE was grounded during switching tests. After SET and RESET voltages were obtained from 5 samples, they were used for a statistical analysis and to train machine learning algorithms. Four classification models, K-nearest Neighbors [18], Support Vector Machine [19], Decision Trees [20] and Random Forest classifier [21] were applied for data processing and prediction.

3. Results and discussion

Fig. 2(a-e) showed typical current–voltage (I-V) characteristics of honey RRAM devices from each sample. The bias voltage was swept at a rate of 1 V/s. A current compliance of 10 μA was applied in the SET process to prevent dielectric breakdown of the honey film. All 5 devices exhibit forming-free bipolar resistive switching behaviors. In positive voltage sweep, current increased gradually till compliance at the SET voltage (V_{set}), which indicates the change of the honey thin film from high resistance state (HRS) to low resistance state (LRS). In negative voltage sweep, current compliance was removed and the current maintained at a high level since the honey film was still at LRS but dropped abruptly when the bias reached the RESET voltage (V_{reset}), when the honey film changed from LRS back to HRS. As summarized in Fig. 2(f), these 5 devices have different V_{set} and V_{reset} and therefore different values of read memory window (V_{set}-V_{reset}) in which the device can be "read" without changing the memory state. The currents in HRS, I_{HRS} measured at the read voltage which is 1/10 or larger of V_{set}, were also different. Such difference can be attributed to their different BE and drying temperature and duration of the honey film.

As a mixture of sugars and other carbohydrates, honey is mainly fructose (about 38 %) and glucose (about 32 %). Current conduction in honey-based RRAM can be potentially explained by formation and rapture of conductive filaments as in RRAM devices based on glucose [12] and glucose [13]. The proposed resistive switching mechanism is schematically presented in Fig. 3. During drying of the honey film, the thermal energy was sufficiently high to break covalently bonded backbone molecules of glucose and fructose chains to form numerous structural defects in the pristine honey film. These structural defects acted as shallow trap centers. Main chemical functional groups such as –OH group originated from either water and/or polysaccharides compounds in honey such as glucose, fructose, sucrose, etc. and C—O group from monosaccharides compounds also dissociated from polysaccharides of honey. These functional groups also formed interstitial spaces to trap charges. The defect sites by structural defects and interstitial traps are shown Fig. 3(a). Under the positive bias in HRS, Al atoms from the top electrode oxidized to Al ions which drifted along the bulk honey film through these defect sites toward the bottom electrode [Fig. 3(b)] under the electric field. When reaching the bottom ITO or Cu_xO/Cu electrode, Al ions reduced to Al atoms and stacked up [Fig. 3(c)]. At V_{set}, Al atoms reached the top electrode and formed a continuous path by conductive filaments for current conduction [Fig. 3(d)], and honey-RRAM transited from HRS to LRS. As the voltage sweep was reversed with negative bias on the top Al electrode, LRS was maintained until voltage equaled V_{reset} when filaments were ruptured [Fig. 3(e)] due to Joule heating. Since defect sites in the honey film play a key role for drifting of Al ions in the filament formation process, and drying temperatures and durations of the honey film affect the concentration of structural defects, this mechanism can be used to explain those different switching characteristics of honey-RRAMs due to different drying conditions in Fig. 2. The effect of Cu_xO and ITO bottom electrode is still under investigation. One potential explanation is attributed to Cu_xO since it was reported that Cu_xO film also has resistive switching properties [22].

To investigate each design in Fig. 1(c), up to 100 devices on each sample were tested, and statistical analysis on SET and RESET voltages of the 5 samples was applied. Fig. 4 summarized the probability of the V_{set} and V_{reset} values in different voltage ranges from each sample using probability density function (PDF), a useful tool to show the likelihood that random variables fall within a particular range of values. As shown in Fig. 4, the 5 samples clearly demonstrated different characteristics of peak value and width of the curve, indicating that different process conditions in Fig. 1(c) have impact on the resistive switching behaviors of the devices. Clear peak values are shown for each sample which indicates that a relatively large number of measurements fall into the corresponding voltage ranges.

Statistical results in Fig. 4 showed that the process conditions clearly

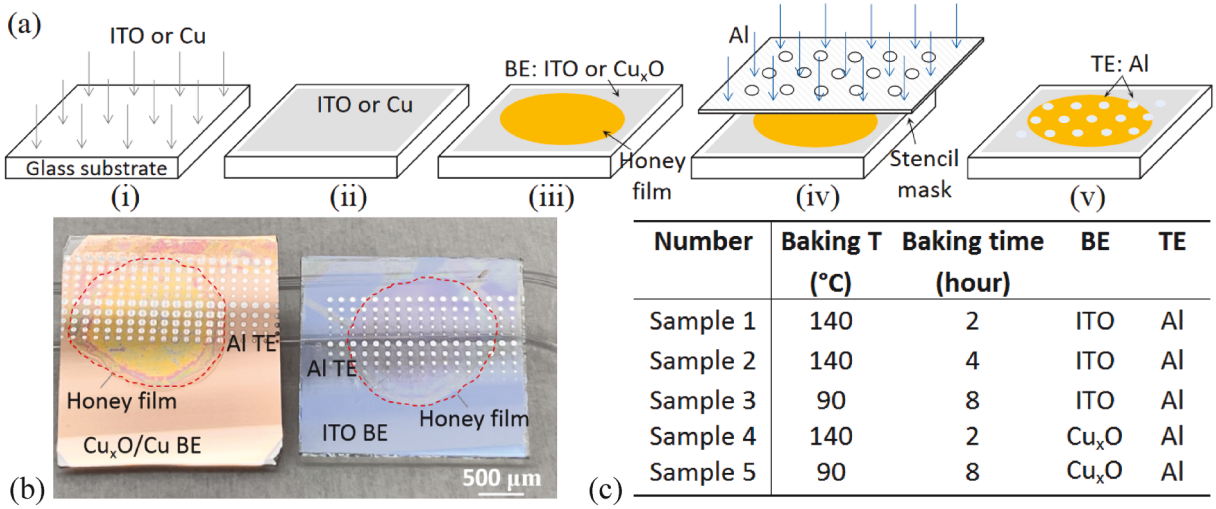

(c)

Number	Baking T (°C)	Baking time (hour)	BE	TE
Sample 1	140	2	ITO	Al
Sample 2	140	4	ITO	Al
Sample 3	90	8	ITO	Al
Sample 4	140	2	Cu_xO	Al
Sample 5	90	8	Cu_xO	Al

Fig. 1. (a) Schematic process flow of Al/honey/ITO and Al/honey/Cu_xO/Cu RRAMs: (i) deposition of ITO or Cu on glass substrate, (ii) after ITO and Cu deposition, (iii) spin coating and baking honey film on ITO or Cu_xO, (iv) deposition of Al through a stencil mask, (v) finished device. (b) Photographs of honey RRAMs with Cu_xO/Cu or ITO BE and Al TE. (c) Summary of sample numbers and process conditions.

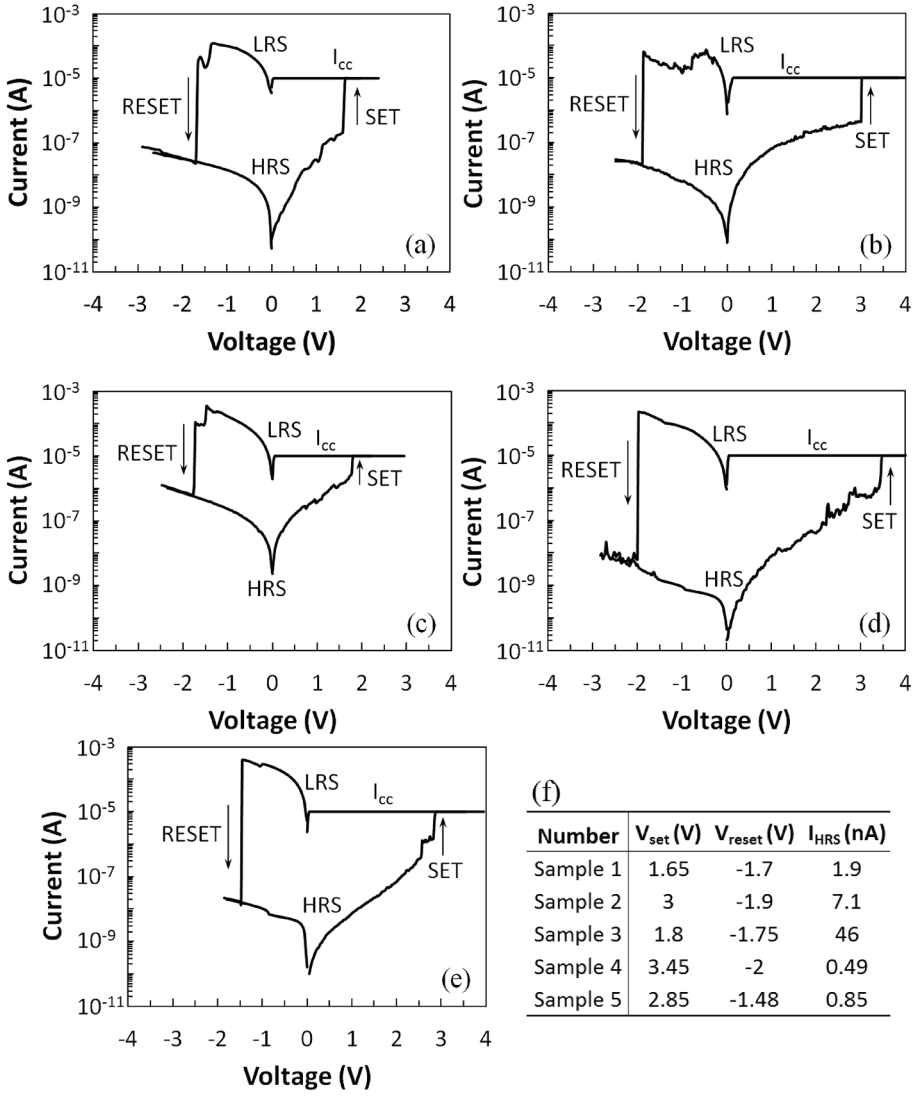

(f)

Number	V_{set} (V)	V_{reset} (V)	I_{HRS} (nA)
Sample 1	1.65	-1.7	1.9
Sample 2	3	-1.9	7.1
Sample 3	1.8	-1.75	46
Sample 4	3.45	-2	0.49
Sample 5	2.85	-1.48	0.85

Fig. 2. Bipolar resistive switching characteristics of 5 honey-RRAM devices from each sample: (a) sample 1, (b) sample 2, (c) sample 3, (d) sample 4 and (e) sample 5. (f) Summary of V_{set}, V_{reset} and I_{HRS} of the devices in (a)-(e).

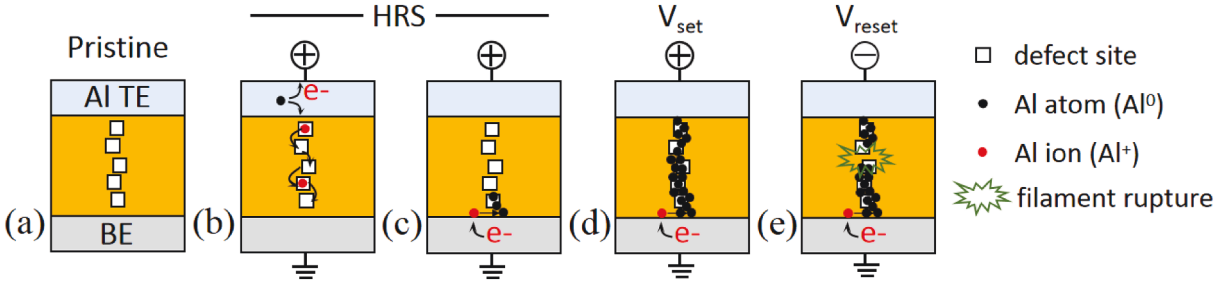

Fig. 3. Resistive switching mechanism of honey-RRAM: (a) pristine device after fabrication with defect sites in the honey film, (b) Al^0 oxidized to Al^+ which drifted to BE through defect sites, (c) Al^+ reduced to Al^0 at BE and stacked up, and Al filaments were (d) formed at V_{set} and (e) ruptured at V_{reset}.

impact resistive switching characteristics of devices. Therefore, predicting the optimal process conditions is critical. To the end, machine learning techniques were applied to make such predictions by formulating the problem into a binary classification. The machine learning model takes the process conditions as input to predict whether the target value falls in a pre-defined specific range. Specifically in this study, the input features included the bottom electrode material, the top electrode material, baking temperature and duration, as in Fig. 1(c). The focused targets were SET and RESET voltage. The classification models used to process the data included K-nearest Neighbors [18], Support Vector Machine [19], Decision Trees [20] and Random Forest classifier [21]. These models were chosen because they represent different classification algorithms. K-nearest Neighbors is a voting-based classification where results are computed by a majority vote of the k nearest neighbors of each data point. Support Vector Machine generates a hyperplane which separates different classes. Decision Trees produce a set of rules to

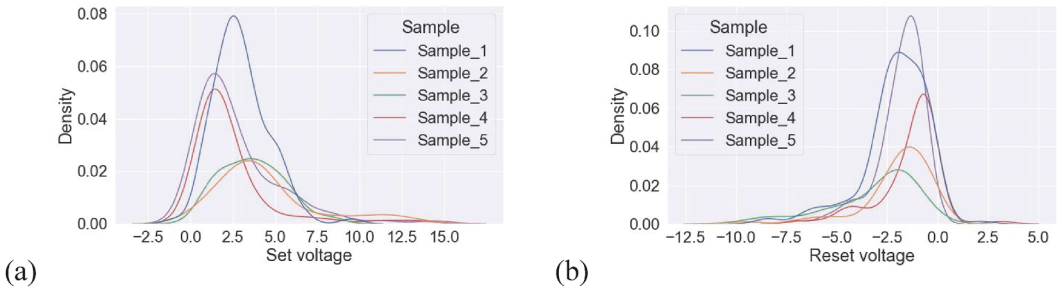

Fig. 4. Per-sample probability density functions (PDF) for (a) SET voltage and (b) RESET voltage.

classify data. Random Forest classifier is a *meta*-estimator that utilizes multiple decision trees to make predictions.

For SET voltage, the range of [0 V, 6 V] was applied as the target range for testing purposes, and this range can be adjusted based on the needs of the prediction. The k-fold cross validation (k = 4) was used in the model. As an example, Fig. 5 showed the analysis results using the model of K-nearest Neighbors. The performance of the machine learning model was stable across 5 samples and baking conditions. Notably, the prediction accuracy for data points at a baking time of 4 h was slightly lower than others as shown in Fig. 5(c), which was consistent with the per-sample accuracy for sample 2 in Fig. 5(a). Machine learning methods are data-driven, and collecting sufficient amount of data required for training has been a well-known challenge in research domains such as microfabrication and material science [23]. Due to the fact that sample 2 is the only sample which was baked for 4 h, the training data for this particular baking time is limited. Nonetheless, the overall performance of the machine learning model demonstrated an average accuracy close or above 90 %. The per-sample, per-temperature, and per-baking time accuracy of the K-nearest Neighbor model is shown in Fig. 5(d). The learning results by 4 classification models were summarized in Fig. 5(d) with similar performance and accuracy ranging from 89.9 % to 91.6 %. This testified the potential of leveraging machine learning techniques to predict device switching characteristics, and comparing to the traditional trial-and-error approach, machine learning is more efficient in process development. To further improve the accuracy of prediction, a larger scale of training dataset with more process

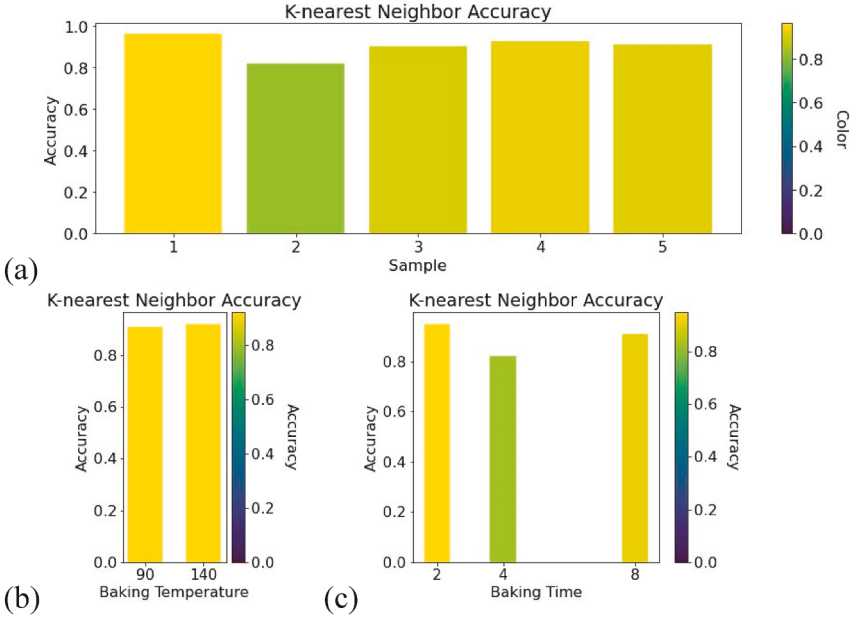

Per sample accuracy					Per temp. accuracy		Per baking time accuracy		
1	2	3	4	5	90	140	2	4	8
96.4%	82%	90%	92.4%	91.3%	90.8%	92%	94.9%	82%	90.8%

(d)

Classification Model	K-nearest Neighbors	Support vector machine	Decision trees	Random forest
Accuracy	89.9%	91.6%	91.6%	91.6%

(e)

Fig. 5. Classification performance of K-n.earest neighbors: (a) accuracy vs samples; (b) accuracy vs baking temperature; (c) accuracy vs baking time. (d) Summary of K-nearest Neighbors accuracy. (e) Summary of the accuracy of 4 classification models on predicting SET voltages.

conditions and a hybrid approach combining machine learning and statistical modeling are currently under investigation.

As suggested by extensive studies in the literature [24,25], the accuracy of machine learning algorithms is largely dependent on the quality and size of the training samples. In many research fields, including microfabrication, collecting training data is costly. Therefore, training machine learning models with a moderate amount of data is ideal. In this paper, we were able to achieve high accuracy (~90 %) with a small dataset. There are still rooms for further improvement such as training the models with a bigger dataset by more process conditions and voltage values from more devices, etc. which are currently under investigation.

4. Conclusion

Process conditions and resistive switching characteristics of natural organic RRAM were correlated through experimental study and machine learning. Bottom electrodes, drying temperature and duration of the honey films were varied by 5 combinations to fabricate honey RRAM devices, with SET and RESET voltages from up to 100 devices of each process condition measured and used to train machine learning algorithms. Four classification models of K-nearest Neighbors, Support Vector Machine, Decision Trees and Random Forest classifier were applied to process the data and accuracy of 89.9 % to 91.6 % were obtained for predicting SET voltage.

Declaration of Competing Interest

The authors declare that they have no known competing financial interests or personal relationships that could have appeared to influence the work reported in this paper.

Data availability

Data will be made available on request.

Acknowledgments

Feng Zhao and Xinghui Zhao acknowledge the support from the National Science Foundation, United States (ECCS-2104976).

References

[1] Le Gallo M, Sebastian A. An overview of phase-change memory device physics. J Phys D Appl Phys 2020;53:213002. https://doi.org/10.1088/1361-6463/ab7794.
[2] Shi T, Wang R, Wu ZH, Sun YZ, An JJ, Liu Q. A review of resistive switching devices: performance improvement, characterization, and applications. Small Struct 2021;2:2000109. https://doi.org/10.1002/sstr.202000109.
[3] Tang JS, Bishop D, Kim SY, Copel M, Gokmen TF, Todorov T, et al. ECRAM as Scalable Synaptic Cell for High-Speed. IEEE International Electron Devices Meeting (IEDM): Low-Power Neuromorphic Computing; 2018. https://ieeexplore.ieee.org/document/8614551.
[4] Bertolazzi S, Bondavalli P, Roche S, San T, Choi SY, Colombo L, et al. Nonvolatile memories based on graphene and related 2D materials. Adv Mater 2019;31:1806663. https://doi.org/10.1002/adma.201806663.
[5] Hota MK, Bera MK, Kundu B, Kundu SC, Maiti CK. A natural silk fibroin protein-based transparent bio-memristor. Adv Funct Mater 2012;22:4493–9. https://doi.org/10.1002/ADFM.201200073.
[6] Chang YC, Wang YH. Resistive switching behavior in gelatin thin films for nonvolatile memory application. ACS Appl Mater Interfaces 2014;6:5413–21. https://doi.org/10.1021/AM500815N.
[7] Chen YC, Yu HC, Huang CY, Chung WL, Wu SL, Su YK. Nonvolatile bio-memristor fabricated with egg albumen film. Sci Rep 2015;5:1–12. https://doi.org/10.1038/srep10022.
[8] Hosseini NR, Lee JS. Biocompatible and flexible chitosan-based resistive switching memory with magnesium electrodes. Adv Funct Mater 2015;25:5586–92. https://doi.org/10.1002/ADFM.201502592.
[9] Nagashima K, Koga H, Celano U, Zhuge F, Kanai M, Rahong S, et al. Cellulose nanofiber paper as an ultra flexible nonvolatile memory. Sci Rep 2014;4:1–7. https://doi.org/10.1038/srep05532.
[10] Raeis-Hosseini N, Lee JS. Controlling the resistive switching behavior in starch-based flexible biomemristors. ACS Appl Mater Interfaces 2016;8:7326–32. https://doi.org/10.1021/ACSAMI.6B01559.
[11] Lim ZX, Cheong KY. Effects of drying temperature and ethanol concentration on bipolar switching characteristics of natural Aloe vera-based memory devices. Phys Chem Chem Phys 2015;17:26833–53. https://doi.org/10.1039/C5CP04622J.
[12] Park SP, Tak YJ, Kim HJ, Lee JH, Yoo H, Kim HJ. Analysis of the bipolar resistive switching behavior of a biocompatible glucose film for resistive random access memory. Adv Mater 2018;30:1800722. https://doi.org/10.1002/ADMA.201800722.
[13] Xing Y, Sueoka B, Cheong KY, Zhao F. Nonvolatile resistive switching memory based on monosaccharide fructose film. Appl Phys Lett 2021;119:163302. https://doi.org/10.1063/5.0067453.
[14] Da Silva PM, Gauche C, Gonzaga LV, Costa ACO, Fett R. Honey: chemical composition, stability and authenticity. Food Chem 2016;196:309–23. https://doi.org/10.1016/J.FOODCHEM.2015.09.051.
[15] Sivkov AA, Xing Y, Cheong KY, Zeng X, Zhao F. Investigation of honey thin film as a resistive switching material for nonvolatile memories. Mater Lett 2020;271:127796. https://doi.org/10.1016/J.MATLET.2020.127796.
[16] Sueoka B, Cheong KY, Zhao F. Study of synaptic properties of honey thin film for neuromorphic systems. Mater Lett 2022;308:131169. https://doi.org/10.1016/J.MATLET.2021.131169.
[17] Kim H, Hwang S, Sueoka B, Zhao F. Memristive synaptic device based on a natural organic material—honey for spiking neural network in biodegradable neuromorphic systems. J Phys D Appl Phys 2022;55:225105. https://doi.org/10.1088/1361-6463/AC585B.
[18] Peterson L. K-nearest neighbor. Scholarpedia 2009;4:1883. 10.4249/scholarpedia.1883.
[19] Noble WS. What is a support vector machine? Nat Biotechnol 2006;24:1565–7. https://doi.org/10.1038/nbt1206-1565.
[20] Kingsford C, Salzberg SL. What are decision trees? Nat Biotechnol 2008;26:1011–3. https://doi.org/10.1038/nbt0908-1011.
[21] Pal M. Random forest classifier for remote sensing classification. Int J Remote Sens 2005;26:217–22. https://doi.org/10.1080/01431160412331269698.
[22] Rehman S, Hur JH, Kim DK. Resistive switching in solution-processed copper oxide (Cu_xO) by stoichiometry tuning. J Phys Chem C 2018;122:11076–85. https://doi.org/10.1021/acs.jpcc.8b00432.
[23] Zhang Y, Ling C. A strategy to apply machine learning to small datasets in materials science. NPJ Comput Mater 2018;4:1–8. https://doi.org/10.1038/s41524-018-0081-z.
[24] Tam VH, Kabbara S, Yeh RF, Leary RH. Impact of sample size on the performance of multiple-model pharmacokinetic simulations. Antimicrob Agents Chemother 2006;50:3950–2. https://doi.org/10.1128/AAC.00337-06.
[25] Kalayeh HM, Landgrebe DA. Predicting the required number of training samples. IEEE Trans Pattern Anal Mach Intell 1983;6:664–7. https://doi.org/10.1109/TPAMI.1983.4767459.

Feng Zhao received his PhD degree in Electrical Engineering from University of Colorado at Boulder. He is currently an associate professor of electrical engineering at the School of Engineering and Computer Science, Washington State University, Vancouver, WA, USA. His research focuses on natural organic materials based memory and artificial synaptic devices for biodegradable neuromorphic systems, wide bandgap semiconductors, MEMS/NEMS, solar cells, microneedle and neural interface devices.